

# Identification of Functional and Expression Polymorphisms Associated With Risk for Antineutrophil Cytoplasmic Autoantibody–Associated Vasculitis

Peter A. Merkel,<sup>1</sup> Gang Xie,<sup>2</sup> Paul A. Monach,<sup>3</sup> Xuemei Ji,<sup>4</sup> Dominic J. Ciavatta,<sup>5</sup>  
Jinyoung Byun,<sup>4</sup> Benjamin D. Pinder,<sup>2</sup> Ai Zhao,<sup>2</sup> Jinyi Zhang,<sup>6</sup> Yohannes Tadesse,<sup>2</sup> David Qian,<sup>4</sup>  
Matthew Weirauch,<sup>7</sup> Rajan Nair,<sup>8</sup> Alex Tsoi,<sup>8</sup> Christian Pagnoux,<sup>9</sup> Simon Carette,<sup>9</sup>  
Sharon Chung,<sup>10</sup> David Cuthbertson,<sup>11</sup> John C. Davis Jr.,<sup>12</sup> Paul F. Dellaripa,<sup>13</sup> Lindsay Forbess,<sup>14</sup>  
Ora Gewurz-Singer,<sup>8</sup> Gary S. Hoffman,<sup>15</sup> Nader Khalidi,<sup>16</sup> Curry Koenig,<sup>17</sup>  
Carol A. Langford,<sup>15</sup> Alfred D. Mahr,<sup>18</sup> Carol McAlear,<sup>1</sup> Larry Moreland,<sup>19</sup> E. Philip Seo,<sup>20</sup>  
Ulrich Specks,<sup>21</sup> Robert F. Spiera,<sup>22</sup> Antoine Sreih,<sup>1</sup> E. William St.Clair,<sup>23</sup> John H. Stone,<sup>24</sup>  
Steven R. Ytterberg,<sup>21</sup> James T. Elder,<sup>25</sup> Jia Qu,<sup>26</sup> Toshiki Ochi,<sup>27</sup> Naoto Hirano,<sup>27</sup>  
Jeffrey C. Edberg,<sup>28</sup> Ronald J. Falk,<sup>5</sup> Christopher I. Amos,<sup>4</sup> and Katherine A. Siminovitch,<sup>6</sup>  
for the Vasculitis Clinical Research Consortium

Supported by the Erna Baird Memorial Grant, the Vasculitis Foundation, the Ontario Research Fund (grant RE-05075), the University of Toronto Department of Medicine Challenge Grant, and the National Natural Science Foundation of China (grant 31270930). Dr. Siminovitch holds a tier 1 Canada Research Chair and the Sherman Family Chair in Genomic Medicine. The Vasculitis Clinical Research Consortium (VCRC) has received support from the NIH (National Institute of Arthritis and Musculoskeletal and Skin Diseases grants U54-AR-057319 and R01-AR-047799, National Center for Research Resources grant U54-RR-019497, the Office of Rare Diseases Research, and the National Center for Advancing Translational Sciences). The VCRC is part of the Rare Diseases Clinical Research Network.

<sup>1</sup>Peter A. Merkel, MD, MPH, Carol McAlear, MA, Antoine Sreih, MD: University of Pennsylvania, Philadelphia; <sup>2</sup>Gang Xie, MD, PhD, Benjamin D. Pinder, PhD, Ai Zhao, PhD, Yohannes Tadesse, PhD: Mount Sinai Hospital, Lunenfeld-Tanenbaum Research Institute and Toronto General Research Institute, Toronto, Ontario, Canada; <sup>3</sup>Paul A. Monach, MD, PhD: Boston University and VA Boston Healthcare System, Boston, Massachusetts; <sup>4</sup>Xuemei Ji, MD, PhD, Jinyoung Byun, PhD, David Qian, PhD, Christopher I. Amos, PhD: Dartmouth College, Lebanon, New Hampshire; <sup>5</sup>Dominic J. Ciavatta, PhD, Ronald J. Falk, MD: University of North Carolina, Chapel Hill; <sup>6</sup>Jinyi Zhang, MD, PhD, Katherine A. Siminovitch, MD: Mount Sinai Hospital, Lunenfeld-Tanenbaum Research Institute, Toronto General Research Institute and University of Toronto, Toronto, Ontario, Canada; <sup>7</sup>Matthew Weirauch, PhD: Cincinnati Children's Hospital Medical Center, Cincinnati, Ohio; <sup>8</sup>Rajan Nair, PhD, Alex Tsoi, MS, PhD, Ora Gewurz-Singer, MD: University of Michigan, Ann Arbor; <sup>9</sup>Christian Pagnoux,

MD, MPH, Simon Carette, MD: Mount Sinai Hospital and University of Toronto, Toronto, Ontario, Canada; <sup>10</sup>Sharon Chung, MD: University of California, San Francisco; <sup>11</sup>David Cuthbertson, MS: University of South Florida, Tampa; <sup>12</sup>John C. Davis Jr., MD: University of California, San Francisco; <sup>13</sup>Paul F. Dellaripa, MD: Brigham and Women's Hospital, Boston, Massachusetts; <sup>14</sup>Lindsay Forbess, MD: Cedars-Sinai Medical Center, West Hollywood, California; <sup>15</sup>Gary S. Hoffman, MD, Carol A. Langford, MD, MHS: Cleveland Clinic, Cleveland, Ohio; <sup>16</sup>Nader Khalidi, MD: McMaster University, Hamilton, Ontario, Canada; <sup>17</sup>Curry Koenig, MD: University of Utah, Salt Lake City; <sup>18</sup>Alfred D. Mahr, MD, PhD: Hôpital Saint-Louis, Paris, France; <sup>19</sup>Larry Moreland, MD: University of Pittsburgh, Pittsburgh, Pennsylvania; <sup>20</sup>E. Philip Seo, MD, MHS: Johns Hopkins University, Baltimore, Maryland; <sup>21</sup>Ulrich Specks, MD, Steven R. Ytterberg, MD: Mayo Clinic, Rochester, Minnesota; <sup>22</sup>Robert F. Spiera, MD: Hospital for Special Surgery, New York, New York; <sup>23</sup>E. William St.Clair, MD: Duke University Medical Center, Durham, North Carolina; <sup>24</sup>John H. Stone, MD, MPH: Massachusetts General Hospital, Boston; <sup>25</sup>James T. Elder, MD, PhD: University of Michigan and Ann Arbor VA Hospital, Ann Arbor, Michigan; <sup>26</sup>Jia Qu, MD: Wenzhou Medical University, Wenzhou, China; <sup>27</sup>Toshiki Ochi, PhD, Naoto Hirano, MD, PhD: University of Toronto and Princess Margaret Cancer Centre, Toronto, Ontario, Canada; <sup>28</sup>Jeffrey C. Edberg, PhD: University of Alabama at Birmingham.

Drs. Amos and Siminovitch contributed equally to this work.

Address correspondence to Katherine A. Siminovitch, MD, Mount Sinai Hospital, LTRI, Room 778D, 600 University Avenue, Toronto, Ontario M5G 1X5, Canada. E-mail: ksimin@mshri.on.ca

Submitted for publication September 8, 2016; accepted in revised form December 20, 2016.

**Objective.** To identify risk alleles relevant to the causal and biologic mechanisms of antineutrophil cytoplasmic antibody (ANCA)-associated vasculitis (AAV).

**Methods.** A genome-wide association study and subsequent replication study were conducted in a total cohort of 1,986 cases of AAV (patients with granulomatosis with polyangiitis [Wegener's] [GPA] or microscopic polyangiitis [MPA]) and 4,723 healthy controls. Meta-analysis of these data sets and functional annotation of identified risk loci were performed, and candidate disease variants with unknown functional effects were investigated for their impact on gene expression and/or protein function.

**Results.** Among the genome-wide significant associations identified, the largest effect on risk of AAV came from the single-nucleotide polymorphism variants rs141530233 and rs1042169 at the *HLA-DPBI* locus (odds ratio [OR] 2.99 and OR 2.82, respectively) which, together with a third variant, rs386699872, constitute a triallelic risk haplotype associated with reduced expression of the *HLA-DPBI* gene and HLA-DP protein in B cells and monocytes and with increased frequency of complementary proteinase 3 (PR3)-reactive T cells relative to that in carriers of the protective haplotype. Significant associations were also observed at the *SERPINA1* and *PTPN22* loci, the peak signals arising from functionally relevant missense variants, and at *PRTN3*, in which the top-scoring variant correlated with increased *PRTN3* expression in neutrophils. Effects of individual loci on AAV risk differed between patients with GPA and those with MPA or between patients with PR3-ANCAs and those with myeloperoxidase-ANCAs, but the collective population attributable fraction for these variants was substantive, at 77%.

**Conclusion.** This study reveals the association of susceptibility to GPA and MPA with functional gene variants that explain much of the genetic etiology of AAV, could influence and possibly be predictors of the clinical presentation, and appear to alter immune cell proteins and responses likely to be key factors in the pathogenesis of AAV.

Granulomatosis with polyangiitis (Wegener's) (GPA) and microscopic polyangiitis (MPA) are life-threatening necrotizing vasculitides that are strongly associated with the presence of antineutrophil cytoplasmic antibodies (ANCAs) reactive to proteinase 3 (PR3) or myeloperoxidase (MPO). Although often considered a single disease, GPA and MPA diverge in important respects, such as in the extent of their association with PR3-reactive ANCAs compared to MPO-reactive ANCAs, the risk of relapsing disease, and the association of GPA with granulomatous inflammation. The etiology of AAV remains unknown; however, genome-wide association studies

(GWAS) performed in a North American GPA cohort and a European GPA/MPA cohort confirmed the findings from candidate gene analyses identifying strong associations of these diseases with major histocompatibility complex (MHC) class II region alleles (1,2). A genome-wide significant association at the *SERPINA1* locus was also identified in the European cohort study, with both this and several associations with MHC alleles being differentially detected between patient subsets defined by the presence of PR3-ANCAs or MPO-ANCAs (2).

These findings have not yet been replicated, and knowledge remains rudimentary regarding the non-MHC loci and specific disease-causal variants predisposing to GPA and/or to MPA. Therefore, we sought to further define the genetic variation underpinning the susceptibility to GPA and MPA by conducting a new GWAS and a validation study of a larger, independently ascertained North American-based cohort of GPA/MPA patients and healthy controls, involving functional annotation of the risk loci to identify candidate disease-causal alleles.

## PATIENTS AND METHODS

**Subjects.** All study subjects were of self-reported European ancestry, with the diagnosis of AAV, and specifically of GPA or MPA, being based on the American College of Rheumatology modified criteria for the classification of vasculitis (3). The discovery cohort included the following subjects: 779 AAV cases recruited via 13 centers from the Vasculitis Clinical Research Consortium (VCRC), which conducts studies involving vasculitis patients in the US, Canada, and elsewhere; 438 AAV cases recruited via the Wegener's Granulomatosis Genetic Repository (WGGER), a study conducted at 8 centers in the US from 2001 to 2005; and 378 AAV cases from the University of North Carolina Kidney Center (key clinical and serologic features are provided in Supplementary Table 1, available on the *Arthritis & Rheumatology* web site at <http://onlinelibrary.wiley.com/doi/10.1002/art.40034/abstract>). The controls included 202 healthy subjects recruited from the WGGER, and 3,121 historic controls whose genotype data were obtained from the Resource for Genetic Epidemiology Research on Aging study (4,5). The replication cohort included 505 AAV cases and 1,477 healthy controls recruited independently from Canada and the US via a Toronto-based AAV study, and 114 independent cases recruited via the VCRC. Demographic data and samples of peripheral blood cells and/or saliva were obtained from all subjects after their provision of written informed consent. The local institutional review boards approved the study.

**Genotyping methods.** For the GWAS, 1,615 AAV cases and 202 healthy controls were genotyped at the Mount Sinai Hospital Clinical Genomics Centre, and 3,121 historic controls were genotyped at Affymetrix (Santa Cruz, CA) using the Axiom Biobank 1 Genotyping array. This array tests 628,679 single-nucleotide polymorphisms (SNPs), including 246,000 genome-wide association markers (36.5%), 265,000 nonsynonymous coding SNPs (39.3%), 70,000 loss-of-function SNPs (10.4%), 23,000 expression quantitative trait loci (eQTL) SNPs (3.4%), 2,000 pharmacogenetic markers (0.3%), and 27,679 "custom" markers. Genotypes were

called and processed using Affymetrix Genotyping Console version 4.2 and SNPfilter software. Quality control filtering was performed using Golden Helix SVS software (version 8.3.4) and with a genotype call rate of >95%, individual sample call rate of >97%, and exclusion of SNPs with a Hardy-Weinberg equilibrium (HWE)  $P$  value of  $<10^{-5}$ . After filtering, genotypes derived from SNP markers common to both data sets were merged in a single file containing 1,528 cases, 3,309 controls, and 333,040 SNPs. A set of linkage disequilibrium (LD)-pruned SNPs with a minor allele frequency (MAF) of >5% was used to estimate identity by descent (ibd) and ancestry. For each pair of individuals with an estimated ibd of >0.25, the sample with the lower call rate was removed. Principal components analysis was used to exclude samples from subjects with non-European ancestry (6). In total, 1,371 cases, 3,258 controls, and 333,035 SNPs passed quality control filters (see Supplementary Figure 1, available on the *Arthritis & Rheumatology* web site at <http://onlinelibrary.wiley.com/doi/10.1002/art.40034/abstract>).

For the replication study, 8 SNPs in 6 gene loci were genotyped in 619 AAV cases and 1,477 controls using Sequenom iPLEX assays. One other SNP (rs62132293) at the *PRTN3* locus was genotyped using TaqMan (Applied Biosystems). After quality control filtering, 615 cases, 1,465 controls, and 9 SNPs were retained for analysis. For the replication study of the patients with MPO-ANCAs/perinuclear ANCAs (designated herein as MPO-ANCAs), 3 additional SNPs (rs3998159, rs7454108, and rs1049072) at the *HLA-DQA2* and *DQB1* loci were genotyped on the same platform. The GWAS and replication data sets were then combined for meta-analysis.

**Statistical analysis.** *Association tests and meta-analyses.* For the discovery data set, case-control association tests were conducted using logistic regression, with the principal components differing between cases and controls included as covariates, to adjust for population stratification. Calculation of the genomic control factor using EigenStrat showed a minimal inflation value of 1.012 and 0.991 before and after adjustment for the top 3 eigenvectors, respectively (see Supplementary Figure 2, <http://onlinelibrary.wiley.com/doi/10.1002/art.40034/abstract>). An analysis of all of the nonzero eigenvalues established that 221,341 independent tests were conducted from 280,677 autosomal markers, which, with Bonferroni correction, established the  $P$  value for genome-wide significance as  $<2.2 \times 10^{-7}$ .

Meta-analysis of the data from the GWAS and replication logistic regression analyses was conducted using the basic meta-analysis function in Plink version 1.9 (6,7). Differences between patients with GPA and patients with MPA and between patients with PR3-ANCAs/cytoplasmic ANCAs (designated herein as PR3-ANCAs) and those with MPO-ANCAs were studied using this approach. Between-study heterogeneity was tested by the chi-square-based Cochran's  $Q$  statistic. Heritability was estimated using genome-wide complex trait analysis, as described by Lee et al (8), and assuming an AAV prevalence of 1/10,000. Prior to this analysis, we excluded sex chromosome data, SNPs with MAFs of <0.05 and missing rates of >0.01, individuals whose missing SNP rates were >0.01, SNPs with an HWE  $P$  value of <0.05, or markers with a significant difference in missingness between cases and controls.

*Imputation.* Genome-wide imputation for the 4,629 samples in the discovery cohort was performed using 1000 Genomes Project Phase 3 data as the reference (release date October 2014) for the autosomes, and Phase 1 data (release date

August 2012) as the reference for the X chromosome. Following removal of SNPs with call rates of <95%, MAFs of <0.001, and HWE  $P$  values of  $<10^{-5}$ , SHAPEIT ([http://shapeit.v2.r790.Ubuntu\\_12.04.4.static](http://shapeit.v2.r790.Ubuntu_12.04.4.static)) was used to derive phased genotypes, and the phased data were imputed using IMPUTE version 2 ([http://impute.v2.3.2\\_x86\\_64\\_static](http://impute.v2.3.2_x86_64_static)) to assess ~5-Mb nonoverlapping intervals (9). Imputation within defined regions was performed using IMPUTE version 2 without prephasing.

*Conditional analysis.* To test for multiple independent effects within the HLA region, a logistic regression framework was used to assess individual HLA alleles for association, including the top 3 principal components as covariates to account for population stratification. After we had identified the most significant marker, we tested for additional independent effects by including the dose of the top markers in a joint model. Conditional analysis was performed using the proc logistic module of SAS (version 9.2) to obtain odds ratios (ORs) when all top markers were jointly analyzed.

*Population attributable fraction (PAF).* The PAF was estimated using ORs from a multivariate logistic regression model incorporating SNPs from multiple loci, so that each OR is adjusted for the effects of the other SNPs. The PAF for effects from an allele at a single locus was determined as follows:

$$\text{PAF} = \frac{\text{RAF}(\text{OR} - 1)}{1 + \text{RAF}(\text{OR} - 1)}$$

where OR is the odds ratio associated with the allele genotype, and RAF is the allele frequency of the risk variant. For computation over multiple loci, the following formula was used:

$$\text{PAF}_{\text{combined}} = 1 - \left( \prod_{i=1}^{n\text{loci}} 1 - (\text{PAF}_i) \right)$$

*Random forest analysis.* The potential role of combinations of alleles in the risk of AAV was evaluated by random forest analysis using classification and regression tree (CART) methodology (10). Data from 11 risk-associated variants were subjected to analyses in which CARTs were repetitively built using two-thirds of the samples and variables. The CARTs were then used to classify the remaining one-third of the data. Eight variants that improved the model fit by  $\geq 3\%$  were retained to build a CART. The rpart program in R and the Gini index measure were used to identify optimal splits of the data, with the complexity parameter set to 0.001 and the data then pruned to include only those nodes containing at least 20 observations. This final model had a classification accuracy of 73%. ORs were calculated with the following formula:

$$\text{OR} = \frac{\text{cases in node } i / \text{controls in node } i}{\text{cases in node } 1 / \text{controls in node } 1}$$

The Woolf approximation was used to compute standard errors and confidence intervals.

*Functional annotation.* The online Probabilistic Identification of Causal SNPs (PICS) algorithm (<http://www.broadinstitute.org/pubs/finemapping/?q=pics>) was used to identify variants at each risk locus with a PICS probability of >0.0275, consistent with that used by Farh et al (11). We then used the Ensembl Variant Effect Predictor web tool to annotate these variants for predicted functional consequences (<http://www.ensembl.org/info/>

docs/tools/vep/index.html) and used Genevar (12), seeQTL ([http://www.bios.unc.edu/research/genomic\\_software/seeQTL/](http://www.bios.unc.edu/research/genomic_software/seeQTL/)) (13), and the University of Chicago eQTL browser (<http://eqtl.uchicago.edu/cgi-bin/gbrowse/eqtl/>) to identify eQTLs.

**Cellular assays.** Peripheral blood mononuclear cells (PBMCs) and polymorphonuclear leukocytes (obtained from patients at Mount Sinai Hospital) were isolated over Ficoll-Hypaque. For quantitative polymerase chain reaction (qPCR), RNA (500 ng) was reverse transcribed using random hexamer primers and SuperScript III reverse transcriptase (Invitrogen), and qPCR was performed using SYBR Green and the gene-appropriate primer pairs (listed in Supplementary Table 2, <http://onlinelibrary.wiley.com/doi/10.1002/art.40034/abstract>). Samples were run on an ABI Prism 7900HT system (Applied Biosystems), and the fold change in expression of the specific gene relative to the internal control gene (*COX5B* for *PRTN3*; *GAPDH* for *HLA-DPBI*) was calculated using the  $2^{-\Delta\Delta C_t}$  method (14).

For flow cytometry, PMBCs were stained with phycoerythrin-conjugated anti-CD19 antibodies, allophycocyanin-Cy7-conjugated anti-CD14 antibodies (BD Biosciences), and/or fluorescein isothiocyanate (FITC)-conjugated HLA-DP antibodies (Leinco) or FITC-conjugated murine IgG (BD Biosciences). The cells were then analyzed using a FACSCanto cytometer (BD Biosciences) and FlowJo software.

For ELISpot experiments, 20-mer peptides, which were selected using published data or the NetMHCII version 2.2 prediction algorithm (<http://www.cbs.dtu.dk>), were synthesized and purified by the manufacturer (Genscript) (for details, see Supplementary Table 3, <http://onlinelibrary.wiley.com/doi/10.1002/art.40034/abstract>).

PBMCs ( $2 \times 10^{-5}$ ) from PR3-ANCA-positive vasculitis patients and healthy controls were suspended in 20% fetal bovine serum-supplemented RPMI and incubated in 96-well ELISpot plates (Millipore) precoated with an anti-human interferon- $\gamma$  (IFN $\gamma$ ) monoclonal antibody (eBioscience). Cells were stimulated for 24 hours at 37°C with 10  $\mu$ g/ml peptide or 1  $\mu$ g/ml concanavalin A (Sigma) and incubated with a biotinylated mouse anti-human IFN $\gamma$  antibody (eBioscience), avidin-horseradish peroxidase (eBioscience), and aminoethylcarbazole solution (BD ELISpot), and an ImmunoSpot reader and software (Cellular Technology) were used to detect IFN $\gamma$ -releasing cells.

## RESULTS

**GPA/MPA susceptibility loci.** After filtering and correction for population substructure, our GWAS discovery data set included 333,035 SNPs genotyped in 1,371 subject with AAV (GPA or MPA) and 3,258 healthy controls, with no evidence of inflation of the test statistic ( $\lambda_{GC} = 0.991$ ) (see Supplementary Figures 1 and 2 and Supplementary Table 1, <http://onlinelibrary.wiley.com/doi/10.1002/art.40034/abstract>).

Association analysis of this cohort identified 120 SNPs across the MHC class II locus achieving genome-wide significance levels, with the strongest signals emanating from the *DPBI*, *DPAI*, *DQAI*, and *DQBI* genes (Table 1 and Supplementary Table 4 [<http://onlinelibrary.wiley.com/doi/10.1002/art.40034/abstract>]).

Four other SNPs across 3 non-MHC gene loci also achieved genome-wide significance levels and were taken forward, together with 5 top-scoring SNPs from the MHC region, for a replication study in an independent cohort of 615 cases and 1,465 controls (Table 1; details also shown in Supplementary Figure 1 and Supplementary Table 1 [<http://onlinelibrary.wiley.com/doi/10.1002/art.40034/abstract>]). Because all of the associations tested were replicated (at a threshold of  $P \leq 0.05$ ), the GWAS and replication data sets were combined for a meta-analysis, and the 9 associations were also explored in patient subgroups defined by GPA or MPA phenotypes or by ANCA specificities and/or immunofluorescence patterns (PR3-ANCAs or MPO-ANCAs).

Results of the meta-analysis confirmed the MHC class II region as the locus most strongly associated with AAV susceptibility (Table 1). The peak association signals arose from 2 *HLA-DPBI* gene variants, rs141530233 ( $P = 1.13 \times 10^{-89}$ ) and rs1042169 ( $P = 1.12 \times 10^{-84}$ ), with other significant associations observed in the *HLA-DPAI*, *DQAI*, and *DQBI* genes (Table 1; see also Supplementary Figures 3 and 4 [<http://onlinelibrary.wiley.com/doi/10.1002/art.40034/abstract>]). Associations with *DPAI* and *DPBI* remained strong in the GPA and PR3-ANCA subgroups, but not in the MPA or MPO-ANCA subgroups. Conversely, the *DQBI* association was much stronger in patients with MPO-ANCAs compared to those with PR3-ANCAs (Table 2). In view of this divergence, a GWAS, replication analysis, and meta-analysis were also performed de novo to compare patients with either PR3-ANCAs or MPO-ANCAs to healthy controls. These analyses revealed significant associations of the MPO-ANCA phenotype with the variants rs3998159 ( $P = 5.24 \times 10^{-25}$ ) and rs7454108 ( $P = 5.03 \times 10^{-25}$ ) at the *HLA-DQA2* locus (Table 3). Neither this association nor any other significant associations beyond those detected in the AAV total cohort GWAS were detected in the subset GWAS analysis of PR3-ANCA-positive AAV cases and healthy controls (results available in Supplementary Tables 5 and 6, <http://onlinelibrary.wiley.com/doi/10.1002/art.40034/abstract>).

Among the non-MHC associations identified in the total AAV GWAS, the strongest signal arose from a SNP (rs28929474) in the *SERPINA1* gene ( $P = 3.09 \times 10^{-12}$ ) encoding an  $\alpha 1$  anti-trypsin null (“Z”) allele that was previously implicated in GPA by candidate gene analysis (Table 1; see also Supplementary Figures 3 and 4 [<http://onlinelibrary.wiley.com/doi/10.1002/art.40034/abstract>]) (15). This association was limited to the GPA and PR3-ANCA subsets (Table 2) and is consistent with prior GWAS data showing that a significant association with another *SERPINA1* SNP, rs7151526, depended entirely on the concomitant presence of the Z allele (2).

A significant association of AAV with rs62132293, a SNP located 2.6 kb upstream of the *PRTN3* transcription start site, was also observed ( $P = 8.60 \times 10^{-11}$ ); this finding is in keeping with previously observed associations at this locus (albeit with different SNPs) in AAV candidate gene and GWAS analyses (Table 1 and Supplementary Figures 3 and 4 [<http://onlinelibrary.wiley.com/doi/10.1002/art.40034/abstract>]) (2,16). This association was limited to the GPA and PR3-ANCA subsets (Table 2), consistent with the pathophysiologic relevance of the *PRTN3*-encoded PR3 serine protease to these phenotypes (17).

Significant associations with AAV were observed at the *PTPN22* rs6679677 and rs2476601 loci ( $P = 1.88 \times 10^{-8}$  and  $P = 1.86 \times 10^{-7}$ , respectively) (Table 1 and Supplementary Figures 3 and 4 [<http://onlinelibrary.wiley.com/doi/10.1002/art.40034/abstract>]). Consistent with their equivalent effect sizes, these variants are in almost complete LD ( $r^2 = 0.99$ ). However, the rs2476601 variant encodes an Arg620Trp substitution in the Lyp phosphatase associated with risk of multiple autoimmune diseases, including giant cell arteritis (18,19). Although not consistently observed in candidate gene studies (20,21), the association of rs2476601 with GPA/MPA is strongly supported by our data, and unlike most of the other significant associations observed, this allele's strength of association did not differ between the subgroups (Table 2).

The discovery GWAS of either the entire cohort or the PR3-ANCA subgroup revealed no reliable associations at the *SEMA6A* gene locus, possibly because those analyses involved a different case-control cohort. In the current discovery GWAS, there were 189 SNPs identified in the 1-MB region around *SEMA6A*, of which the most significant variant, rs12521259, was located ~100 kb upstream of *SEMA6A* ( $P$  for association =  $9.11 \times 10^{-3}$  in the full cohort and  $P = 4.87 \times 10^{-3}$  in the PR3-ANCA subgroup).

Analyses of the associations in patient subgroups defined by the presence or absence of lung or kidney disease revealed a modest association with AAV risk at the *HLA-DPA1* locus in patients with kidney involvement ( $P = 8.15 \times 10^{-3}$ ), whereas no significant subgroup differences were apparent at the other risk loci (results in Supplementary Table 7, <http://onlinelibrary.wiley.com/doi/10.1002/art.40034/abstract>). Modest associations with *HLA-DPBI* and *HLA-DPA1* were observed but restricted to the patients with ANCA-positive AAV; this finding may be a reflection of the relatively low numbers of ANCA-negative cases analyzed.

**Contribution of risk alleles jointly to disease susceptibility.** As the strongest associations in all subgroups were with MHC gene SNPs, independence of the individual allele associations was explored by forward logistic regression selection analysis. Beginning with the most

significant SNP identified in the total cohort or in the PR3-ANCA or MPO-ANCA subgroups, additional significant variants were incorporated into the analysis until no variants significant at the  $P < 5 \times 10^{-8}$  level remained. This analysis revealed that variants in several of the class II genes studied in each group were jointly significantly associated with AAV risk (results in Supplementary Table 8, <http://onlinelibrary.wiley.com/doi/10.1002/art.40034/abstract>).

These analyses showed that the array heritability of AAV was a mean  $\pm$  SD  $0.2197 \pm 0.0204$ , while in analyses with the HLA region removed, the array heritability was  $0.138 \pm 0.022$ . The PAF for the risk loci to disease was also assessed, and the collective contribution of these loci to risk of AAV was found to be substantive (PAF of 77%), albeit variable (PAFs between 30% and 87%) across different the subgroups (Table 4).

The extent to which the risk variants/variant combinations might be predictive of disease was also evaluated using random forest and CART methods. These analyses confirmed the strong association of HLA class II alleles with AAV risk (details in Supplementary Figure 5, <http://onlinelibrary.wiley.com/doi/10.1002/art.40034/abstract>). Furthermore, homozygosity for the relatively common *DPBI* risk allele rs141530233 and *DPA1* risk allele rs9277341, together with homozygosity or heterozygosity for the rare *SERPINA1* risk variant rs2829474, identified a subgroup of individuals with an OR of  $>10$  for developing AAV.

For HLA alleles, no subsets were defined by heterozygotes, and further modeling comparing the goodness-of-fit of additive, dominant, and recessive models showed that the risk imbued by the *HLA-DPBI*, *DPA1*, and *DQAI* disease-associated variants is recessively inherited, i.e., conferred by carriage of the common homozygous genotypes (see Supplementary Table 9, <http://onlinelibrary.wiley.com/doi/10.1002/art.40034/abstract>). Associations of the homozygous risk genotypes with AAV were as follows: OR of 3.58 for rs141530233, OR of 2.69 for rs9277341, and OR of 1.80 for rs352425282. Similar results were found for the subgroups defined by carriage of PR3-ANCAs or MPO-ANCAs, with recessive models fitting best. These observations suggest a potential for genetic data to inform the distinction of patient subsets within the AAV population and identify an unusual recessive effect for the HLA region loci studied.

**Disease-associated *PRTN3* polymorphism identified as a novel eQTL.** To identify candidate causal variants, additional genotypes were imputed and the PICS algorithm was applied across each risk locus (11). Although peak association signals at a few loci were stronger for imputed SNPs than for observed SNPs (details in Supplementary Table 10, <http://onlinelibrary.wiley.com/doi/10.1002/art.40034/abstract>), among all variants with a PICS probability of  $>0.0275$ , the

**Table 1.** Results of GWAS, replication, and combined analyses of associations with antineutrophil cytoplasmic autoantibody-associated vasculitis\*

SNP	Locus	Position	Gene	Risk allele	GWAS				Replication analysis				Combined analysis			
					RAF		P <sup>†</sup>	OR (95% CI) <sup>‡</sup>	RAF		P <sup>§</sup>	OR (95% CI)	P <sup>‡</sup>		OR (95% CI)	
					Cases	Controls			Cases	Controls			Cases	Controls		
rs141530233	6p21.32	33048688	<i>HLA-DPB1</i>	A del <sup>¶</sup>	0.86	0.70	$5.93 \times 10^{-56}$	2.76 (2.44-3.13)	0.90	0.69	$2.45 \times 10^{-39}$	4.00 (3.23-5.00)	$1.13 \times 10^{-89}$	2.99 (2.69-3.33)		
rs1042169	6p21.32	33048686	<i>HLA-DPB1</i>	G	0.86	0.70	$4.41 \times 10^{-52}$	2.57 (2.27-2.94)	0.90	0.68	$1.94 \times 10^{-39}$	4.00 (3.23-5.00)	$1.12 \times 10^{-84}$	2.82 (2.54-3.13)		
rs9277341	6p21.32	33039625	<i>HLA-DPA1</i>	T	0.84	0.70	$1.62 \times 10^{-40}$	2.21 (1.96-2.50)	0.87	0.66	$3.58 \times 10^{-34}$	3.13 (2.63-3.70)	$6.09 \times 10^{-71}$	2.44 (2.21-2.69)		
rs35242582	6p21.32	32600057	<i>HLA-DQA1</i>	A	0.82	0.74	$3.34 \times 10^{-16}$	1.61 (1.43-1.79)	0.82	0.74	$3.59 \times 10^{-8}$	1.59 (1.35-1.89)	$6.34 \times 10^{-23}$	1.60 (1.46-1.76)		
rs1049072	6p21.32	32634355	<i>HLA-DQB1</i>	A	0.23	0.17	$4.23 \times 10^{-10}$	1.43 (1.28-1.59)	0.21	0.17	$1.69 \times 10^{-3}$	1.30 (1.10-1.54)	$6.46 \times 10^{-13}$	1.40 (1.28-1.53)		
rs6679677	1p13.2	114303808	<i>PTPN22</i>	A	0.13	0.09	$2.40 \times 10^{-8}$	1.49 (1.30-1.72)	0.11	0.09	$4.57 \times 10^{-2}$	1.25 (1.00-1.55)	$1.88 \times 10^{-8}$	1.40 (1.25-1.57)		
rs62132293	19p13.3	838178	<i>PRTN3</i>	G	0.37	0.31	$5.55 \times 10^{-8}$	1.30 (1.18-1.43)	0.37	0.31	$6.81 \times 10^{-5}$	1.33 (1.15-1.52)	$8.60 \times 10^{-11}$	1.29 (1.19-1.39)		
rs28929474	14q32.13	94844947	<i>SERPINA1</i>	T	0.04	0.02	$8.26 \times 10^{-8}$	2.09 (1.59-2.73)	0.04	0.02	$6.72 \times 10^{-5}$	2.18 (1.49-3.20)	$3.09 \times 10^{-12}$	2.18 (1.75-2.71)		
rs2476601	1p13.2	114377568	<i>PTPN22</i> ( <i>R620W</i> )	A	0.13	0.10	$3.03 \times 10^{-7}$	1.45 (1.26-1.66)	0.11	0.09	$5.38 \times 10^{-2}$	1.24 (1.00-1.53)	$1.86 \times 10^{-7}$	1.36 (1.21-1.53)		

\* RAF = risk allele frequency; OR = odds ratio; 95% CI = 95% confidence interval.

† EigenStrat P value.

‡ P values for the replication analysis and combined genome-wide association study (GWAS) data sets were calculated using the Cochran-Mantel-Haenszel method, which combines allele frequency counts.

§ Plink P value.

¶ The single-nucleotide polymorphism (SNP) rs141530233 is an insertion/deletion polymorphism, with the risk genotype lacking an adenosine residue at nucleotide position 33048688 (adenosine deletion [A del]) and the nonrisk genotype containing this adenosine residue.

**Table 2.** MHC and non-MHC associations with ANCA-associated vasculitis according to clinically and serologically defined subgroups of patients\*

SNP	Locus	Gene	Risk allele	Overall analysis of combined cohort (n = 1,986 cases, n = 4,723 controls)				Clinical syndrome						ANCA specificity					
				P <sup>†</sup>	OR	GPA (n = 1,556) vs. controls (n = 4,723)	MPA (n = 236) vs. controls (n = 4,723)	GPA (n = 1,556) vs. MPA (n = 236)	PR3-cANCA (n = 1,361) vs. controls (n = 4,723)	MPO-pANCA vs. controls (n = 4,723)	PR3-cANCA (n = 1,361) vs. controls (n = 4,723)	MPO-pANCA vs. controls (n = 4,723)	PR3-cANCA (n = 1,361) vs. MPO-pANCA (n = 378)	PR3-cANCA (n = 1,361) vs. controls (n = 4,723)	MPO-pANCA vs. controls (n = 4,723)	PR3-cANCA (n = 1,361) vs. MPO-pANCA (n = 378)	PR3-cANCA (n = 1,361) vs. controls (n = 4,723)	MPO-pANCA vs. controls (n = 4,723)	PR3-cANCA (n = 1,361) vs. MPO-pANCA (n = 378)
rs141530233	6p21.32	<i>HLA-DPB1</i>	A del	1.13 × 10 <sup>-89</sup>	2.99	3.80 × 10 <sup>-93</sup>	9.45 × 10 <sup>-5</sup>	1.58	1.45 × 10 <sup>-9</sup>	1.33 × 10 <sup>-106</sup>	1.50 × 10 <sup>-2</sup>	1.50 × 10 <sup>-2</sup>	1.50 × 10 <sup>-2</sup>	1.50 × 10 <sup>-2</sup>	1.50 × 10 <sup>-2</sup>	1.50 × 10 <sup>-2</sup>	1.50 × 10 <sup>-2</sup>	3.53 × 10 <sup>-32</sup>	
rs1042169	6p21.32	<i>HLA-DPB1</i>	G	1.12 × 10 <sup>-84</sup>	2.82	1.09 × 10 <sup>-90</sup>	2.22 × 10 <sup>-3</sup>	1.40	9.50 × 10 <sup>-12</sup>	6.53 × 10 <sup>-106</sup>	1.27 × 10 <sup>-1</sup>	1.27 × 10 <sup>-1</sup>	1.27 × 10 <sup>-1</sup>	1.27 × 10 <sup>-1</sup>	1.27 × 10 <sup>-1</sup>	1.27 × 10 <sup>-1</sup>	1.27 × 10 <sup>-1</sup>	3.44 × 10 <sup>-36</sup>	
rs9277341	6p21.32	<i>HLA-DPA1</i>	T	6.09 × 10 <sup>-71</sup>	2.44	2.78 × 10 <sup>-73</sup>	9.40 × 10 <sup>-4</sup>	1.45	4.96 × 10 <sup>-7</sup>	4.52 × 10 <sup>-84</sup>	3.61 × 10 <sup>-3</sup>	3.61 × 10 <sup>-3</sup>	3.61 × 10 <sup>-3</sup>	3.61 × 10 <sup>-3</sup>	3.61 × 10 <sup>-3</sup>	3.61 × 10 <sup>-3</sup>	3.61 × 10 <sup>-3</sup>	4.55 × 10 <sup>-20</sup>	
rs35242582	6p21.32	<i>HLA-DQA1</i>	A	6.34 × 10 <sup>-23</sup>	1.60	1.60 × 10 <sup>-20</sup>	8.91 × 10 <sup>-3</sup>	1.36	1.36 × 10 <sup>-1</sup>	5.78 × 10 <sup>-18</sup>	2.34 × 10 <sup>-7</sup>	2.34 × 10 <sup>-7</sup>	2.34 × 10 <sup>-7</sup>	2.34 × 10 <sup>-7</sup>	2.34 × 10 <sup>-7</sup>	2.34 × 10 <sup>-7</sup>	2.34 × 10 <sup>-7</sup>	7.67 × 10 <sup>-1</sup>	
rs1049072	6p21.32	<i>HLA-DQB1</i>	A	6.46 × 10 <sup>-13</sup>	1.40	1.40 × 10 <sup>-7</sup>	4.16 × 10 <sup>-9</sup>	1.89	2.99 × 10 <sup>-3</sup>	3.82 × 10 <sup>-3</sup>	2.13 × 10 <sup>-24</sup>	2.13 × 10 <sup>-24</sup>	2.13 × 10 <sup>-24</sup>	2.13 × 10 <sup>-24</sup>	2.13 × 10 <sup>-24</sup>	2.13 × 10 <sup>-24</sup>	2.13 × 10 <sup>-24</sup>	7.53 × 10 <sup>-13</sup>	
rs6679677	1p13.2	<i>PTPN22</i>	A	1.88 × 10 <sup>-8</sup>	1.40	2.38 × 10 <sup>-7</sup>	8.96 × 10 <sup>-4</sup>	1.58	5.48 × 10 <sup>-1</sup>	7.89 × 10 <sup>-6</sup>	8.83 × 10 <sup>-7</sup>	8.83 × 10 <sup>-7</sup>	8.83 × 10 <sup>-7</sup>	8.83 × 10 <sup>-7</sup>	8.83 × 10 <sup>-7</sup>	8.83 × 10 <sup>-7</sup>	8.83 × 10 <sup>-7</sup>	1.08 × 10 <sup>-1</sup>	
rs62132293	19p13.3	<i>PRTN3</i>	G	8.60 × 10 <sup>-11</sup>	1.29	7.06 × 10 <sup>-11</sup>	1.12 × 10 <sup>-1</sup>	1.17	2.70 × 10 <sup>-1</sup>	3.59 × 10 <sup>-13</sup>	5.66 × 10 <sup>-1</sup>	5.66 × 10 <sup>-1</sup>	5.66 × 10 <sup>-1</sup>	5.66 × 10 <sup>-1</sup>	5.66 × 10 <sup>-1</sup>	5.66 × 10 <sup>-1</sup>	5.66 × 10 <sup>-1</sup>	3.22 × 10 <sup>-5</sup>	
rs28929474	14q32.13	<i>SERPINA1</i>	T	3.09 × 10 <sup>-12</sup>	2.18	3.53 × 10 <sup>-13</sup>	2.06 × 10 <sup>-2</sup>	1.88	3.86 × 10 <sup>-1</sup>	1.29 × 10 <sup>-13</sup>	4.96 × 10 <sup>-3</sup>	4.96 × 10 <sup>-3</sup>	4.96 × 10 <sup>-3</sup>	4.96 × 10 <sup>-3</sup>	4.96 × 10 <sup>-3</sup>	4.96 × 10 <sup>-3</sup>	4.96 × 10 <sup>-3</sup>	1.92 × 10 <sup>-1</sup>	
rs2476601	1p13.2	<i>PTPN22 (R620W)</i>	A	1.86 × 10 <sup>-7</sup>	1.36	1.77 × 10 <sup>-6</sup>	1.31 × 10 <sup>-3</sup>	1.56	4.95 × 10 <sup>-1</sup>	3.19 × 10 <sup>-5</sup>	5.85 × 10 <sup>-6</sup>	5.85 × 10 <sup>-6</sup>	5.85 × 10 <sup>-6</sup>	5.85 × 10 <sup>-6</sup>	5.85 × 10 <sup>-6</sup>	5.85 × 10 <sup>-6</sup>	5.85 × 10 <sup>-6</sup>	1.40 × 10 <sup>-1</sup>	

\* MHC = major histocompatibility complex; ANCA = antineutrophil cytoplasmic autoantibody; GPA = granulomatosis with polyangiitis (Wegener's); MPA = microscopic polyangiitis; PR3 = proteinase 3; cANCA = cytoplasmic ANCA; MPO = myeloperoxidase; pANCA = perinuclear ANCA; SNP = single-nucleotide polymorphism; OR = odds ratio; A del = adenosine deletion.  
 † EigenStrat P value.



**Table 4.** Population risk estimates for disease-associated SNPs at the MHC and non-MHC loci in all patients with AAV and in clinically and serologically defined subgroups of patients\*

Gene	SNP	RAF	ANCA specificity												
			Combined AAV cohort				Clinical syndrome				PR3-cANCA			MPO-pANCA	
			OR	PAF	OR	PAF	OR	PAF	OR	PAF	OR	PAF			
<i>HLA-DPB1</i>	rs141530233	0.70	2.36	0.49	3.01	0.58	1.64	0.31	3.98	0.68	1.01	0.00			
<i>HLA-DPA1</i>	rs9277341	0.70	1.62	0.30	1.81	0.36	1.26	0.00	1.84	0.37	1.03	0.00			
<i>HLA-DQA1</i>	rs35242582	0.74	1.39	0.22	1.46	0.26	1.06	0.00	1.27	0.17	1.02	0.00			
<i>HLA-DQB1</i>	rs1049072	0.17	1.33	0.05	1.19	0.00	1.91	0.13	1.16	0.00	2.64	0.22			
<i>PRTN3</i>	rs62132293	0.31	1.27	0.08	1.30	0.09	1.18	0.00	1.59	0.16	1.10	0.00			
<i>SERPINA1</i>	rs28929474	0.02	2.13	0.02	2.43	0.02	1.98	0.00	3.64	0.04	2.98	0.00			
<i>PTPN22 (R620W)</i>	rs2476601	0.10	1.45	0.04	1.47	0.04	1.62	0.06	1.71	0.06	2.18	0.10			
Total	-	-	-	0.77	-	0.83	-	0.43	-	0.87	-	0.30			

\* Population risk estimates included the risk allele frequency (RAF), odds ratio (OR), and population attributable fraction (PAF) calculated in the overall combined cohort of patients with antineutrophil cytoplasmic autoantibody (ANCA)-associated vasculitis (AAV), in the clinical subgroups of patients with granulomatosis with polyangiitis (Wegener's) (GPA) and those with microscopic polyangiitis (MPA), and in the serologically defined subgroups of patients with proteinase 3 (PR3)-cytoplasmic ANCA (cANCA) and those with myeloperoxidase (MPO) perinuclear ANCA. SNPs = single-nucleotide polymorphisms; MHC = major histocompatibility complex.

index SNPs derived from direct genotyping were consistently associated with the highest PICS values (see Supplementary Table 11, <http://onlinelibrary.wiley.com/doi/10.1002/art.40034/abstract>). PICS values were particularly high for the index SNPs at the *HLA-DPB1*, *SERPINA1*, and *PTPN22* loci, all of which are functional missense variants (15,22,23). The candidate causal variants at the other HLA gene loci were either synonymous, intronic, or upstream gene variants, but the majority of these noncoding variants, and even several *HLA-DPB1* coding variants, have been annotated as eQTLs that influence gene expression in immune cell lineages (24).

None of the candidate variants at the *PRTN3* locus were coding or reported eQTL SNPs. Increases in *PRTN3* expression levels have, however, been observed in neutrophils from patients with AAV and implicated in the pathogenicity of AAV (17,25). Because knowledge of neutrophil-specific eQTLs remains limited, we evaluated the lead SNP at this locus (rs62132293) for allelic effects on *PRTN3* expression in neutrophils. Results of qPCR analyses revealed cellular *PRTN3* transcript levels to be significantly higher in those homozygous for the risk (G) allele than in donors with CC or CG genotypes (Figure 1). These results identify the rs62132293 SNP as an eQTL for *PRTN3* and suggest that the causal variant at this locus engenders risk by its association with increased *PRTN3* expression.

**Association of the rs141530233 risk variant with altered *HLA-DPB1* expression and T cell responses.** Among the candidate causal variants, the *HLA-DPB1* rs141530233 and rs1042169 SNPs had the largest effects on risk, with respective ORs of 2.99 and 2.82 in the primary cohort and respective ORs of 6.19 and 6.09 in the PR3-ANCA subset (Tables 1 and 2). These SNPs are,

respectively, insertion/deletion (-/A) and missense (G/A) polymorphisms that map only 2 basepairs apart in exon 2 of the *HLA-DPB1* gene, with their risk alleles in complete LD in the control cohort and the reference 1000 Genomes Project data sets. In the latter population, these alleles correlate perfectly with another insertion/deletion polymorphic variant, rs386699872 CA/G, 3 basepairs downstream of rs141530233, suggesting that these variants comprise a triallelic risk and nonrisk *HLA-DPB1* haplotype (see Supplementary Figure 6, <http://onlinelibrary.wiley.com/doi/10.1002/>

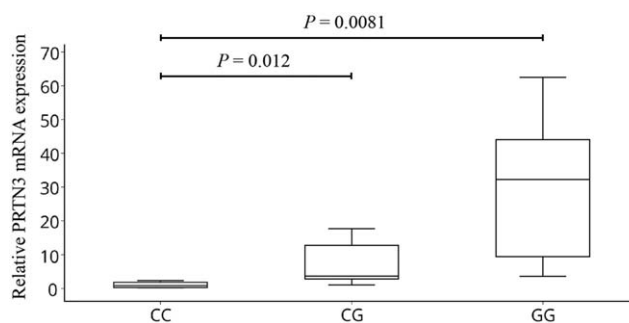


**Figure 1.** Association between the antineutrophil cytoplasmic autoantibody-associated vasculitis variant rs62132293 and increased expression of *PRTN3*. Levels of mRNA for *PRTN3* were measured using quantitative polymerase chain reaction amplification of cDNA from peripheral blood polymorphonuclear leukocytes obtained from healthy donors with the rs62132293 CC genotype (n = 7), rs62132293 CG genotype (n = 9), or rs62132293 GG genotype (n = 6). *PRTN3* expression levels, relative to the values for the calibrator reference gene *COX5B*, are presented as box plots, in which the boxes represent the 25th to 75th percentiles, the horizontal line within the boxes indicates the median, and the bars outside the boxes indicate the lowest and highest values. Data are representative of 3 independent experiments. *P* values were determined by unpaired *t*-test.

art.40034/abstract). To confirm the haplotypic relatedness of the 3 variants, we sequenced this region in 100 study subjects who were homozygous for the rs141530233 and rs1042169 markers. Our findings confirmed the organization of the 3 variants in 2 haplotype blocks (as shown in Supplementary Figure 6), which is consistent with the findings in prior studies of a dimorphic polymorphism (GGPM versus DEAV) at the corresponding amino acid positions 84–87 of the HLA-DPB chain (22,26,27).

Effects of the rs141530233 SNP on gene expression have not been reported, but the linked missense rs1042169 G/A SNP has been catalogued as an eQTL, with presence of the homozygous GG genotype being correlated with increased expression of *HLA-DPB1* in PBMCs (24). These variants are in LD with a SNP variant (rs9277534) in the downstream *HLA-DPB1* 3'-untranslated region, for which the homozygous genotype is associated with lower levels of *HLA-DPB1* and HLA-DP expression in immune cells compared to those in subjects with the alternate homozygous genotype (28,29). We therefore assessed the relationship between the triallelic AAV risk haplotype and *HLA-DPB1*/HLA-DP expression using PBMCs from healthy subjects carrying either risk or protective rs1042169 alleles. Results of qPCR analysis revealed *HLA-DPB1* messenger RNA levels to be significantly lower in rs1042169 GG risk allele homozygotes than in subjects with the AA or GA genotypes (Figure 2A).

Furthermore, flow cytometric analyses revealed significantly lower HLA-DP expression on CD19+ B cells and CD14+ monocytes from donors with the GG risk allele than on cells from donors with the GA or AA genotype (Figures 2B and C). Thus, the triallelic risk haplotype defined by the rs1042169 G variant is associated with reduced *HLA-DPB1* transcript levels and HLA-DP surface expression in immune cells.

The finding that a triallelic haplotype was correlated with reduced expression of *HLA-DPB1*/HLA-DP and encoded a putative functionally important HLA-DP polymorphism that is highly associated with risk of AAV, and particularly PR3-ANCA vasculitis, strongly suggests that this genetic variation influences HLA-DP-modulated immune responses that could be relevant to susceptibility.

Because T cells that respond to PR3 protein or peptides have been identified in patients with PR3-ANCA-positive AAV, and because the frequency of T cells responding to a “complementary” peptide encoding anti-sense PR3 codons (cPR3) has been correlated with the presence and activity of disease (30–35), we stimulated PBMCs from patients carrying rs1042169 G and/or A alleles with putatively immunogenic cPR3 and PR3 peptides and used an IFN $\gamma$  ELISpot assay to identify responding T cells. Whereas the PR3 peptides elicited

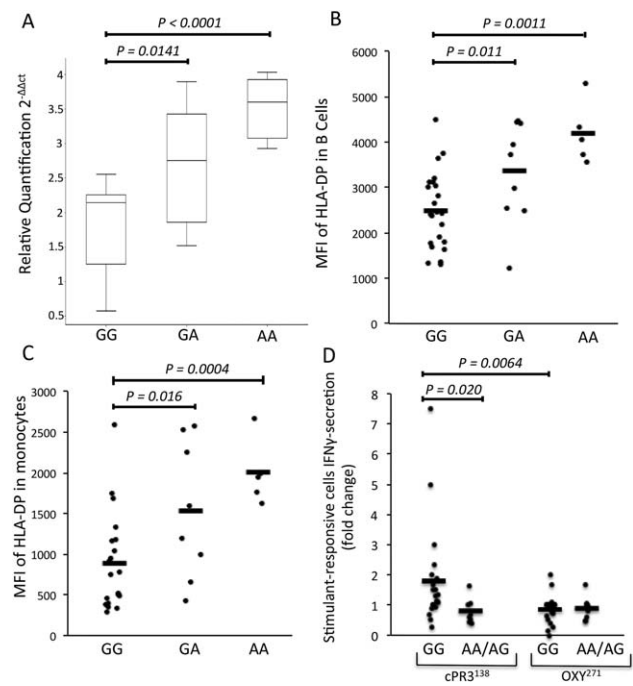


**Figure 2.** Association of the rs1042169 allele with differential *HLA-DPB1* expression and T cell responses. **A**, *HLA-DPB1* mRNA levels were detected by quantitative polymerase chain reaction amplification of cDNA from peripheral blood mononuclear cells (PBMCs) obtained from healthy donors with the rs1042169 GG genotype ( $n = 13$ ), rs1042169 GA genotype ( $n = 8$ ), or rs1042169 AA genotype ( $n = 7$ ). *HLA-DPB1* mRNA levels, relative to the values for the calibrator reference gene *GAPDH*, are shown as box plots, in which the boxes represent the 25th to 75th percentiles, the horizontal line within the boxes indicates the median, and the bars outside the boxes indicate the lowest and highest values. Data are representative of 3 independent experiments. **B** and **C**, Surface HLA-DP levels were evaluated by flow cytometric assay of B cells (**B**) and monocytes (**C**) in anti-DP and anti-CD19 or anti-CD14 antibody-stained PBMCs obtained from donors with the rs1042169 GG genotype ( $n = 24$ ), rs1042169 GA genotype ( $n = 9$ ), or rs1042169 AA genotype ( $n = 5$ ). **D**, PBMCs from patients positive for proteinase 3 (PR3)-specific antineutrophil cytoplasmic autoantibodies who were carriers of the rs10421699 GG genotype ( $n = 21$ ) or the AA/AG genotype ( $n = 8$ ) were stimulated with anti-sense PR3 codons (cPR3) or an OXY control peptide and analyzed by ELISpot for interferon- $\gamma$  (IFN $\gamma$ )-secreting T cells. Results are the mean fold change in stimulated cells relative to unstimulated cells. Symbols in **B–D** represent individual donors; horizontal bars indicate the mean. In **A–C**,  $P$  values were determined by unpaired  $t$ -test. In **D**,  $P$  values were determined by Mann-Whitney U test (GG versus AA/AG + cPR3<sup>138</sup>) or Wilcoxon’s signed rank test (GG cPR3<sup>138</sup> versus GG OXY<sup>271</sup>). MFI = mean fluorescence intensity.

either no response or minimal responses (data not shown), the cPR3 peptide, in most patients, evoked clear reactivity that was completely absent in cells stimulated with an irrelevant (OXY) peptide (Figure 2D) and in cells from healthy controls (data not shown). Frequencies of IFN $\gamma$ -producing cells differed strikingly among patients

according to their rs1042169 allele status, with the numbers of responding T cells being significantly higher ( $P < 0.02$ ) in risk allele homozygotes than in individuals having 1 or 2 copies of the protective A allele, and significantly higher in risk allele homozygotes following stimulation with cPR3 compared to stimulation with OXY ( $P < 0.0064$ ). These findings are consistent with the presence of cPR3-reactive T cells in PR3-ANCA-positive vasculitis patients and suggest the possibility that the altered HLA-DP expression, and possibly function, associated with the *HLA-DPB1* homozygous risk haplotype is correlated with increased numbers of autoreactive cells.

## DISCUSSION

This study identifies MHC and non-MHC gene variants that are associated with GPA/MPA susceptibility and with altered gene expression and/or function of proteins integral to immune responses. Our data reveal that the largest effect on risk emanates from a triallelic *HLA-DPB1* haplotype underpinning a previously reported HLA-DPB amino acid polymorphism across positions 84–87 (22–27). Our data also support major roles for the *PRTN3*, *SERPINA1*, and *PTPN22* genes in AAV susceptibility, providing the first evidence of a genome-wide significant association with the *PTPN22* rs2476601 functional variant, and identifying a correlation of the top-scoring variant at *SERPINA1* as a null allele and at *PRTN3* as an eQTL allele with increased *PRTN3* expression in neutrophils. Results of the CART analysis revealed the potential for these functional variants to be used to identify population subsets of individuals who would be at highly elevated risk of developing GPA or MPA, as indicated by the observed collective PAF of 77%. The estimated array heritability of 21% is comparable to previous estimates of the heritability of inflammatory bowel disease (36).

Among the MHC associations, the *HLA-DPB1* risk haplotype alleles appear particularly significant, having a very strong effect on risk and underpinning a  $\beta$ -chain polymorphism in the HLA-DP antigen-binding pocket that modulates the protein's peptide-binding properties and possibly its effects on T cell allorecognition (22). The physiologic significance of this haplotype can also be inferred on the basis of our data linking these risk alleles to decreased expression of *HLA-DPB1* and HLA-DP and an increased frequency of cPR3 peptide-reactive T cells in patients with anti-PR3 autoantibodies. Although understanding of the autoantigenic epitopes driving T cell responses in AAV is limited, our findings are consistent with prior data correlating alleles at linked *HLA-DPB1* SNP loci to

differential *HLA-DPB1*/HLA-DP expression and with the association of such expression changes, as well as the HLA-DP GGPM/DEAV variance, with differential outcomes of specific immune challenges (28,29). Further investigation is required to define the extent to which the risk haplotype-associated increase in levels of autoreactive T cells reflects the failure to eliminate such cells during thymic selection and/or whether another mechanistic aberrancy may be involved.

Among the non-MHC associations identified, direct causal effects of the *PTPN22* risk variant are strongly suggested by previous data linking the associated Lyp variant to aberrant increases in lymphocyte antigen receptor signaling and dendritic cell activation (23). Direct contribution of the *SERPINA1* rs28929474 risk variant to AAV pathogenesis has also been implied in a study that established a role for  $\alpha_1$ -antitrypsin in inhibiting PR3 protease activity and, by extension, PR3-induced inflammatory responses (37). Similarly, the most strongly associated *PRTN3* variant has been found to increase the neutrophil expression of *PRTN3*, an aberrancy found often in PR3-ANCA-positive patients, and this is correlated with pathogenic neutrophil activation, suggesting that altered *PRTN3* expression mediated via this or another tightly linked variant functionally underpins the *PRTN3* association with AAV (17,38).

Our analyses revealed that the risk associated with the various AAV phenotypes was linked to joint effects of different genes across the HLA class II region. Consistent with a prior study that demonstrated genetic distinctions between PR3-ANCA-positive vasculitis and MPO-ANCA-positive vasculitis (2), we detected peak associations of the *HLA-DPB1* and *HLA-DPA1* variants with positivity for PR3-ANCAs, whereas in those with MPO-ANCAs, the *HLA-DQA2* and *HLA-DQB1* variants showed the strongest associations. Differential effects of these variants also distinguished patients with GPA from those with MPA, suggesting that GPA and PR3-ANCA-positive AAV share a composite set of MHC class II risk alleles that is largely distinct from those conferring risk of MPA and MPO-ANCA-positive AAV. Stronger associations at the *PRTN3* and *SERPINA1* loci appear to distinguish the GPA and PR3-ANCA subsets from their counterpart subgroups. In contrast, effects of the *PTPN22* locus on AAV risk seem equivalent across the different subsets, suggesting that the genetic disparities between subgroups do not reflect insufficient statistical power and are important determinants of phenotypic heterogeneity in AAV.

In summary, our study has illuminated MHC and non-MHC gene variants that are strongly associated with AAV and that are differentially associated with key clinical

and serologic disease subsets. The identified variants could potentially directly influence the pathogenesis of AAV. The extent to which, and the mechanisms whereby, these variants directly cause disease requires more investigation, and our data do not directly preclude the potential biologic relevance of other alleles in LD with these variants, particularly at the *HLA-DPB1* and *PRTN3* loci. Whether the sample size constrained our analysis of important subsets (such as patients with IgG-ANCAs versus those with IgA-ANCAs) or confounded detection of some important associations remains to be determined (39). Nonetheless, our findings identify a set of risk variants that explain much of the genetic risk of GPA/MPA, that appear to influence the clinical presentation of the disease, and that represent biologically important alleles with high potential to drive the aberrant immune responses contributing to the development of AAV.

#### AUTHOR CONTRIBUTIONS

All authors were involved in drafting the article or revising it critically for important intellectual content, and all authors approved the final version to be published. Dr. Siminovitch had full access to all of the data in the study and takes responsibility for the integrity of the data and the accuracy of the data analysis.

**Study conception and design.** Merkel, Xie, Monach, Ciavatta, Pinder, Zhang, Hirano, Edberg, Falk, Amos, Siminovitch.

**Acquisition of data.** Merkel, Xie, Monach, Ji, Ciavatta, Byun, Pinder, Zhao, Zhang, Tadesse, Qian, Weirauch, Nair, Tsoi, Pagnoux, Carette, Chung, Cuthbertson, Davis Jr., Dellaripa, Forbess, Gewurz-Singer, Hoffman, Khalidi, Koenig, Langford, Mahr, McAlear, Moreland, Seo, Specks, Spiera, Sreih, St.Clair, Stone, Ytterberg, Elder, Qu, Ochi, Hirano, Edberg, Falk, Amos, Siminovitch.

**Analysis and interpretation of data.** Merkel, Xie, Monach, Ji, Byun, Pinder, Zhao, Zhang, Tadesse, Weirauch, Chung, Elder, Qu, Ochi, Hirano, Edberg, Amos, Siminovitch.

#### ADDITIONAL DISCLOSURE

Dr. Davis is currently an employee of Pfizer Inc.

#### REFERENCES

- Xie G, Roshandel D, Sherva R, Monach PA, Lu EY, Kung T, et al. Association of granulomatosis with polyangiitis (Wegener's) with HLA-DPB1\*04 and SEMA6A gene variants: evidence from genome-wide analysis. *Arthritis Rheum* 2013;65:2457-68.
- Lyons PA, Rayner TF, Trivedi S, Holle JU, Watts RA, Jayne DR, et al. Genetically distinct subsets within ANCA-associated vasculitis. *N Engl J Med* 2012;367:214-23.
- Fries JF, Hunder GG, Bloch DA, Michel BA, Arend WP, Calabrese LH, et al. The American College of Rheumatology 1990 criteria for the classification of vasculitis: summary. *Arthritis Rheum* 1990;33:1135-6.
- Hoffmann TJ, Zhan Y, Kvale MN, Hesselton SE, Gollub J, Iribarren C, et al. Design and coverage of high throughput genotyping arrays optimized for individuals of East Asian, African American, and Latino race/ethnicity using imputation and a novel hybrid SNP selection algorithm. *Genomics* 2011;98:422-30.
- Banda Y, Kvale MN, Hoffmann TJ, Hesselton SE, Ranatunga D, Tang H, et al. Characterizing race/ethnicity and genetic ancestry for 100,000 subjects in the Genetic Epidemiology Research on Adult Health and Aging (GERA) cohort. *Genetics* 2015;200:1285-95.
- Purcell S, Neale B, Todd-Brown K, Thomas L, Ferreira MA, Bender D, et al. PLINK: a tool set for whole-genome association and population-based linkage analyses. *Am J Hum Genet* 2007;81:559-75.
- Willer CJ, Li Y, Abecasis GR. METAL: fast and efficient meta-analysis of genomewide association scans. *Bioinformatics* 2010;26:2190-1.
- Lee SH, Wray NR, Goddard ME, Visscher PM. Estimating missing heritability for disease from genome-wide association studies. *Am J Hum Genet* 2011;88:294-305.
- Howie BN, Donnelly P, Marchini J. A flexible and accurate genotype imputation method for the next generation of genome-wide association studies. *PLoS Genet* 2009;5:e1000529.
- Breiman L, Friedman J, Olshen RA, Stone CJ. *Classification and Regression Trees*. Belmont, California: Chapman and Hall/CRC; 1984.
- Farh KK, Marson A, Zhu J, Kleinewietfeld M, Housley WJ, Beik S, et al. Genetic and epigenetic fine mapping of causal autoimmune disease variants. *Nature* 2015;518:337-43.
- Yang TP, Beazley C, Montgomery SB, Dimas AS, Gutierrez-Arcelus M, Stranger BE, et al. Genevar: a database and Java application for the analysis and visualization of SNP-gene associations in eQTL studies. *Bioinformatics* 2010;26:2474-6.
- Xia K, Shabalin AA, Huang S, Madar V, Zhou YH, Wang W, et al. seeQTL: a searchable database for human eQTLs. *Bioinformatics* 2012;28:451-2.
- Livak KJ, Schmittgen TD. Analysis of relative gene expression data using real-time quantitative PCR and the  $2^{-\Delta\Delta C_t}$  method. *Methods* 2001;25:402-8.
- Mahr AD, Edberg JC, Stone JH, Hoffman GS, St.Clair EW, Specks U, et al. Alpha<sub>1</sub>-antitrypsin deficiency-related alleles Z and S and the risk of Wegener's granulomatosis. *Arthritis Rheum* 2010;62:3760-7.
- Gencik M, Meller S, Borgmann S, Fricke H. Proteinase 3 gene polymorphisms and Wegener's granulomatosis. *Kidney Int* 2000;58:2473-7.
- Rarok AA, Stegeman CA, Limburg PC, Kallenberg CG. Neutrophil membrane expression of proteinase 3 (PR3) is related to relapse in PR3-ANCA-associated vasculitis. *J Am Soc Nephrol* 2002;13:2232-8.
- Cho JH, Feldman M. Heterogeneity of autoimmune diseases: pathophysiologic insights from genetics and implications for new therapies. *Nat Med* 2015;21:730-8.
- Carmona FD, Mackie SL, Martin JE, Taylor JC, Vaglio A, Eyre S, et al. A large-scale genetic analysis reveals a strong contribution of the HLA class II region to giant cell arteritis susceptibility. *Am J Hum Genet* 2015;96:565-80.
- Jagiello P, Aries P, Arning L, Wagenleiter SE, Csernok E, Hellmich B, et al. The PTPN22 620W allele is a risk factor for Wegener's granulomatosis. *Arthritis Rheum* 2005;52:4039-43.
- Chung SA, Xie G, Roshandel D, Sherva R, Edberg JC, Kravitz M, et al. Meta-analysis of genetic polymorphisms in granulomatosis with polyangiitis (Wegener's) reveals shared susceptibility loci with rheumatoid arthritis. *Arthritis Rheum* 2012;64:3463-71.
- Diaz G, Amicosante M, Jaraquemada D, Butler RH, Guillen MV, Sanchez M, et al. Functional analysis of HLA-DP polymorphism: a crucial role for DPβ residues 9, 11, 35, 55, 56, 69 and 84-87 in T cell allorecognition and peptide binding. *Int Immunol* 2003;15:565-76.
- Zhang J, Zahir N, Jiang Q, Miliotis H, Heyraud S, Meng X, et al. The autoimmune disease-associated PTPN22 variant promotes calpain-mediated Lyp/Pep degradation associated with lymphocyte and dendritic cell hyperresponsiveness. *Nat Genet* 2011;43:902-7.
- The GTEx Consortium. The Genotype-Tissue Expression (GTEx) project. *Nat Genet* 2013;45:580-5.

25. Yang JJ, Pendergraft WF, Alcorta DA, Nachman PH, Hogan SL, Thomas RP, et al. Circumvention of normal constraints on granule protein gene expression in peripheral blood neutrophils and monocytes of patients with antineutrophil cytoplasmic autoantibody-associated glomerulonephritis. *J Am Soc Nephrol* 2004;15:2103–14.
26. Doytchinova IA, Flower DR. In silico identification of super-types for class II MHCs. *J Immunol* 2005;174:7085–95.
27. Silveira LJ, McCanlies EC, Fingerlin TE, van Dyke MV, Mroz MM, Strand M, et al. Chronic beryllium disease, HLA-DPB1, and the DP peptide binding groove. *J Immunol* 2012;189:4014–23.
28. Thomas R, Thio CL, Apps R, Qi Y, Gao X, Marti D, et al. A novel variant marking HLA-DP expression levels predicts recovery from hepatitis B virus infection. *J Virol* 2012;86:6979–85.
29. Petersdorf EW, Malkki M, O’Hugin C, Carrington M, Gooley T, Haagenson MD, et al. High HLA-DP expression and graft-versus-host disease. *N Engl J Med* 2015;373:599–609.
30. Van der Geld YM, Huitema MG, Franssen CF, van der Zee R, Limburg PC, Kallenberg CG. In vitro T lymphocyte responses to proteinase 3 (PR3) and linear peptides of PR3 in patients with Wegener’s granulomatosis (WG). *Clin Exp Immunol* 2000;122:504–13.
31. Winek J, Mueller A, Csernok E, Gross WL, Lamprecht P. Frequency of proteinase 3 (PR3)-specific autoreactive T cells determined by cytokine flow cytometry in Wegener’s granulomatosis. *J Autoimmun* 2004;22:79–85.
32. Popa ER, Franssen CF, Limburg PC, Huitema MG, Kallenberg CG, Tervaert JW. In vitro cytokine production and proliferation of T cells from patients with anti-proteinase 3- and antimyeloperoxidase-associated vasculitis, in response to proteinase 3 and myeloperoxidase. *Arthritis Rheum* 2002;46:1894–904.
33. Pendergraft WF III, Preston GA, Shah RR, Tropsha A, Carter CW Jr, Jennette JC, et al. Autoimmunity is triggered by cPR-3(105–201), a protein complementary to human autoantigen proteinase-3. *Nat Med* 2004;10:72–9.
34. Csernok E, Ai M, Gross WL, Wicklein D, Petersen A, Lindner B, et al. Wegener autoantigen induces maturation of dendritic cells and licenses them for Th1 priming via the protease-activated receptor-2 pathway. *Blood* 2006;107:4440–8.
35. Yang J, Bautz DJ, Lionaki S, Hogan SL, Chin H, Tisch RM, et al. ANCA patients have T cells responsive to complementary PR-3 antigen. *Kidney Int* 2008;74:1159–69.
36. Chen GB, Lee SH, Brion MJ, Montgomery GW, Wray NR, Radford-Smith GL, et al. Estimation and partitioning of (co)heritability of inflammatory bowel disease from GWAS and immunochip data. *Hum Mol Genet* 2014;23:4710–20.
37. Duranton J, Bieth JG. Inhibition of proteinase 3 by  $\alpha$ 1-antitrypsin in vitro predicts very fast inhibition in vivo. *Am J Respir Cell Mol Biol* 2003;29:57–61.
38. Ciavatta DJ, Yang J, Preston GA, Badhwar AK, Xiao H, Hewins P, et al. Epigenetic basis for aberrant upregulation of autoantigen genes in humans with ANCA vasculitis. *J Clin Invest* 2010;120:3209–19.
39. Kelley JM, Monach PA, Ji C, Zhou Y, Wu J, Tanaka S, et al. IgA and IgG antineutrophil cytoplasmic antibody engagement of Fc receptor genetic variants influences granulomatosis with polyangiitis. *Proc Natl Acad Sci U S A* 2011;108:20736–41.